

Dynamics of a periodic tick-borne disease model with co-feeding and multiple patches

Xue Zhang · Bei Sun · Yijun Lou

Received: date / Accepted: date

Abstract By extending a mechanistic model for the tick-borne pathogen systemic transmission with the consideration of seasonal climate impacts, host movement as well as the co-feeding transmission route, this paper proposes a novel modeling framework for describing the spatial dynamics of tick-borne diseases. The net reproduction number for tick growth and basic reproduction number for disease transmission are derived, which predict the global dynamics of tick population growth and disease transmission. Numerical simulations not only verify the analytical results, but also characterize the contribution of co-feeding transmission route on disease prevalence in a habitat and the effect of host movement on the spatial spreading of the pathogen.

Keywords Tick-borne disease · patch model · co-feeding transmission · net reproduction number · basic reproduction number · global stability

1 Introduction

In recent years, tick-borne diseases, including Lyme disease, tick-borne encephalitis, babesiosis and anaplasmosis, are seriously threatening the health of humans living in the countryside or near woodlands. Lyme disease caused by the bacteria pathogen *Borrelia burgdorferi* is the most common tick-borne disease in the northern hemisphere (Kurtenbach et al. 2006). In USA, a total of 33,666 confirmed and probable cases of Lyme disease were reported in

X. Zhang

Department of Mathematics, Northeastern University, Shenyang, 110819, P. R. China

B. Sun

Department of Mathematics, Northeastern University, Shenyang, 110819, P. R. China

Y. Lou

Department of Applied Mathematics, The Hong Kong Polytechnic University, Hung Hom, Kowloon, Hong Kong SAR, P. R. China. Corresponding Author. E-mail: yijun.lou@polyu.edu.hk

2018 and the number of counties with an incidence of ≥ 10 confirmed cases per 100,000 persons increased from 324 in 2008 to 415 in 2018 (CDC 2019). In Europe, there may be more than 200,000 cases per year (O’Connell 2010). In Canada, 992 cases of Lyme disease were reported in 2016 compared with 114 in 2009, and the number of endemic areas is gradually increasing with the expanding range of ticks, which was attributed to climate change (Ogden et al. 2009, 2015).

Several tick-borne diseases are mainly transmitted by *Ixodes* ticks, which are most abundant in forests, woodlands and dense bushes and have three distinct post-egg stages: larva, nymph and adult (Dennis et al. 1998). The development from one stage to the next is processed by taking a blood meal. Immature ticks (larva and nymph) mainly feed on small animals such as rodents and other small vertebrates, and adult ticks prefer large mammals (Ostfeld 2010). Systemic and co-feeding transmissions (also called viraemic and non-viraemic transmissions) are two main routes for the widespread of tick-borne pathogens (Voordouw 2015).

Mathematical models have been formulated to extensively study various aspects of factors involving disease transmission. For example, Rosà et al. (2003) proposed a tick-borne infection dynamics model with two types of host species with differential competence of viraemic transmission, and derived the explicit threshold of disease persistence in terms of viraemic and non-viraemic transmissions. They further explored the impact of the dynamics of tick population and host densities on the persistence of tick-borne disease (Rosà and Pugliese 2007). Zhao (2012) employed a reaction-diffusion model to investigate the global dynamics of Lyme disease based on the reproduction number. Dunn et al. (2013) formulated a mechanistic model of tick-borne pathogens to obtain the specific form of the basic reproduction number, and evaluated the importance of parameters in conformity with the results of global sensitivity analysis. Tick population and tick-borne diseases pose a high level of seasonality, which can also be studied through models with seasonal weather variations. For example, Heffernan, Lou and Wu (2014) developed a tick-borne disease model incorporating climate change and seasonal bird migration and showed that bird migration may amplify the probability of pathogen establishment. Egyed et al. (2012) investigated the seasonal timing of questing by all developmental stages of *Ixodes ricinus* and its infection rate for the major tick-borne pathogens in Hungary. Hancock et al. (2011) proposed an age-structured tick population model and explored seasonal activity patterns of *I. ricinus* for disease persistence subject to temperature changes. Wu et al. (2015) and Liu, Lou and Wu (2017) studied age-structured models with time-dependent periodic maturation delays for tick populations. More models can be found in a brief review (Lou and Wu 2017).

It is well known that natural ecological environment has been separated into many patches due to human activities, such as the construction of highways and railways. Although ticks move only in a small spatial range by themselves, their hosts can freely move among various habitats. Hence, it is interesting and important to investigate the role of host movement on the spread of

tick-borne diseases among different patches. A popular way to describe species movement in a fragmented environment is using the patch modeling framework. For instance, Arino et al. (2005) described a multi-species SEIR epidemic model with spatial dynamics consisting of s species and n patches. Wang and Mulone (2003) proposed an SIS epidemic model between two patches to describe the threshold of disease transmission. Gao and Ruan (2011) formulated an SIS patch model with variable spread coefficients to explore how human movement could affect the transmission of epidemic diseases in patchy environments. Recent extensive theoretical studies have been performed to study asymptotic profiles of the steady states for patch models, see for example, Allen et al. (2007).

Considering the possible impact of patchy environmental, systemic and co-feeding transmission routes and seasonal variations on disease transmission, in this paper, we are going to formulate a tick-borne disease transmission model. The net reproduction number of tick growth and the basic reproduction number for tick-borne pathogen transmission will be derived. Based on these two reproduction numbers, the global dynamics of tick-borne disease model can be characterized. The impact of host movement, co-feeding and seasonal variations on pathogen transmission will be evaluated through numerical simulations.

2 The model

In this section, we will construct a tick-borne disease model with co-feeding transmission in n -patches. Unlike models for tick-borne pathogen transmission reviewed in Lou and Wu (2017), which normally involve many variables, in particular, variables for infected larvae, infected nymphs and so on to capture the main features of stage-structure and infectivity of ticks, here we stratify tick and host populations by their infection status: susceptible (superscript s) and infected (superscript i). Three stages of tick population in an indexed patch (assume to be the k -th patch), larvae (L_k), nymphs (N_k) and adults (A_k) are considered. **The host population in the k -th patch H_k is classified into two distinguished subgroups: susceptible hosts H_k^s and infectious hosts H_k^i .**

The model is formulated based on the following assumptions:

- (i) Since ticks can move by themselves only in a small range and the number of ticks that can be carried from one patch to another through feeding blood is small due to short biting period, we ignore the migration of tick population among n patches.
- (ii) Although many different species can serve as hosts for ticks and competent reservoirs for the pathogen (Ostfeld 2010), as a simplification, we classify them into the rodent compartment and use the averaged parameters in terms of growth, pathogen transmission and movement. We denote $m_{ij}(t)$ as the rodent migration rate from j -th patch to i -th patch.

- (iii) Since transovarial transmission is low in tick population (Pettersson et al. 2014), we assume that all newly emerging larvae are susceptible and pathogen transmission are mainly due to the blood feeding of infectious rodents and/or co-feeding with infectious ticks on a host.
- (iv) Systemic transmission of pathogen involves three closely related paths: susceptible larvae feed on infectious rodents and get infection; infectious larvae develop into infected nymphs; infected nymphs transmit tick-borne pathogens to susceptible rodents through biting on them. Since adults mainly take blood feeding on large-size animals different from hosts for immature ticks, we ignore the transmission between infectious adults and non-viraemic deer (Hudson et al. 1995). **Susceptible nymphs may also get infected through blood feeding on infectious rodents and develop to infectious adults.**
- (v) A susceptible larva can also be infected by co-feeding transmission when it co-feeds on a rodent with an infected nymph in a proximity over a certain period of time. **The co-feeding probability of a susceptible larval tick by infected nymphal ticks depends on the relative location of ticks on the host and the number of infected nymphal ticks. For the simplicity, here we assume that the number of infected ticks is equally distributed on all hosts and do not consider the relative distance between a larva and infected nymphs on one host.** To describe the transmission rate through co-feeding transmission, let η_k be the probability that a susceptible larva gets infection from a co-feeding infected nymph through co-feeding transmission. Assume that feeding nymphs are evenly distributed in all rodents. Since the events that each infectious nymph launches co-feeding transmission to a susceptible larva are independent, the probability that a susceptible larva becomes infected through co-feeding with i number of infectious nymphs is $1 - (1 - \eta_k)^i$ (see Nah et al. (2019) for more details on the derivation).
- (vi) **Tick-borne pathogen transmission via systemic route from infected hosts and that via co-feeding route from infected nymphs are assumed to be independent events. That is, the incidence of one transmission route does not affect the probability of transmission through the other route.**

The transmission routes between multi-stage ticks and rodents can be depicted by the diagram in Fig. 1. Please note that in this diagram, L_k and N_k should be regarded as questing immature ticks looking for host for blood meal. Based on this diagram, a mechanistic model with less variables can be formulated to capture the complex cycle of systematic transmission of the pathogen between the multi-stage ticks and rodents. Considering the birth, stage-structured growth, pathogen transmission and seasonal variations on tick growth and activity, we can formulate the following model for the indexed

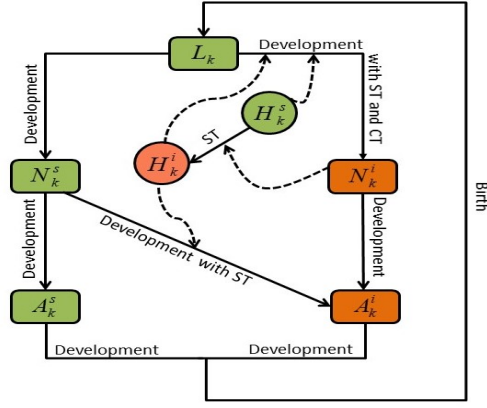


Fig. 1: A schematic illustration of tick-borne disease dynamics with both systemic and co-feeding transmissions: the tick population is stratified into immature ticks (larvae and nymphs) and adults. All newly emerging larvae are assumed to be susceptible, may get infected by taking a blood meal from a host where systemic and co-feeding transmission can both occur, and then develop into nymphs. Susceptible nymphs can also get infection through biting an infectious host. Susceptible hosts can get infection through the bites of infected nymphs. ST: systematic transmission; CT: co-feeding transmission.

k -th patch where $k = 1, 2, \dots, n$:

$$\begin{aligned}
\frac{dL_k(t)}{dt} &= \rho_k(t)A_k(t) - d_k^L(t)L_k(t) - \mu_k^L(t)L_k^2(t) - \beta_k^L(t)H_k(t)L_k(t), \\
\frac{dN_k^s(t)}{dt} &= m_k^L(t)\beta_k^L(t)H_k(t)L_k(t) - d_k^N(t)N_k^s(t) - \mu_k^N(t)N_k(t)N_k^s(t) - \beta_k^N(t)H_k(t)N_k^s(t) \\
&\quad - \zeta_k^L m_k^L(t)\beta_k^L(t)H_k^i(t)L_k(t) - \left(1 - (1 - \eta_k)N_k^i(t)/H_k(t)\right) m_k^L(t)\beta_k^L(t)H_k^s(t)L_k(t) \\
&\quad - \left(1 - (1 - \eta_k)N_k^i(t)/H_k(t)\right) (1 - \zeta_k^L) m_k^L(t)\beta_k^L(t)H_k^i(t)L_k(t), \\
\frac{dN_k^i(t)}{dt} &= \zeta_k^L m_k^L(t)\beta_k^L(t)H_k^i(t)L_k(t) + \left(1 - (1 - \eta_k)N_k^i(t)/H_k(t)\right) m_k^L(t)\beta_k^L(t)H_k^s(t)L_k(t) \\
&\quad + \left(1 - (1 - \eta_k)N_k^i(t)/H_k(t)\right) (1 - \zeta_k^L) m_k^L(t)\beta_k^L(t)H_k^i(t)L_k(t) - d_k^N(t)N_k^i(t) \\
&\quad - \mu_k^N(t)N_k(t)N_k^i(t) - \beta_k^N(t)H_k(t)N_k^i(t), \\
\frac{dA_k^s(t)}{dt} &= m_k^N(t)\beta_k^N(t)H_k(t)N_k^s(t) - d_k^A(t)A_k^s(t) - \mu_k^A(t)A_k(t)A_k^s(t) \\
&\quad - \beta_k^A(t)D_k A_k^s(t) - \zeta_k^N m_k^N(t)\beta_k^N(t)H_k^i(t)N_k^s(t), \\
\frac{dA_k^i(t)}{dt} &= m_k^N(t)\beta_k^N(t)H_k(t)N_k^i(t) + \zeta_k^N m_k^N(t)\beta_k^N(t)H_k^i(t)N_k^s(t) - d_k^A A_k^i(t) \\
&\quad - \mu_k^A(t)A_k(t)A_k^i(t) - \beta_k^A(t)D_k A_k^i(t), \\
\frac{dH_k^s(t)}{dt} &= d_k^H H_k(t) - d_k^H H_k^s(t) - \zeta_k^H \beta_k^N(t)H_k^s(t)N_k^i(t) + \sum_{j=1, j \neq k}^n m_{kj}(t)H_j^s(t) \\
&\quad - \sum_{j=1, j \neq k}^n m_{jk}(t)H_k^s(t), \\
\frac{dH_k^i(t)}{dt} &= \zeta_k^H \beta_k^N(t)H_k^s(t)N_k^i(t) - d_k^H H_k^i(t) + \sum_{j=1, j \neq k}^n m_{kj}(t)H_j^i(t) - \sum_{j=1, j \neq k}^n m_{jk}(t)H_k^i(t),
\end{aligned} \tag{1}$$

where $L_k(t)$ denotes the density of larvae at time t in k -th patch, $N_k^s(t)$ and $N_k^i(t)$ represent the densities of susceptible and infected nymphs at time t in k -th patch, respectively, $A_k^s(t)$ and $A_k^i(t)$ are the densities of susceptible and infected adults at time t in k -th patch. $H_k^s(t)$ and $H_k^i(t)$ are the densities of susceptible and infected hosts in k -th patch at time t , respectively. Please

Table 1: Parameters and descriptions of model (1).

	Parameters	Descriptions	Baseline values
Reproduction	$\rho_k(t)$	Recruitment rate of larvae in k -th patch	see Section 5
Mortality	$d_k^L(t)$	Mortality rate of larvae in k -th patch	$0.01(\text{day}^{-1})$ (Randolph and Rogers (1997))
	$d_k^N(t)$	Mortality rate of nymphs in k -th patch	see Section 5
	$d_k^A(t)$	Mortality rate of adults in k -th patch	$0.00625(\text{day}^{-1})$ (Rosà and Pugliese (2007))
	$\mu_k^L(t)$	Time-dependent parameter with $\mu_k^L L_k$ as the density-dependent death rate of larvae in k -th patch	$10^{-5}(\text{day}^{-1})$ (assumed)
	$\mu_k^N(t)$	Time-dependent parameter with $\mu_k^N N_k$ as the density-dependent death rate of nymphs in k -th patch	$10^{-5}(\text{day}^{-1})$ (assumed)
	$\mu_k^A(t)$	Time-dependent parameter with $\mu_k^A A_k$ as the density-dependent death rate of adults in k -th patch	$10^{-5}(\text{day}^{-1})$ (assumed)
Tick-host encountering	$\beta_k^L(t)$	Encounter rate between larvae and rodents in k -th patch	0.0015 (assumed)
	$\beta_k^N(t)$	Encounter rate between nymphs and rodents in k -th patch	0.00051 (assumed)
	$\beta_k^A(t)$	Encounter rate between adults and deers in k -th patch	0.0001 (assumed)
Molting	$m_k^L(t)$	Molting success rate of larvae developing to nymphs in k -th patch	0.35 (assumed)
	$m_k^N(t)$	Molting success rate of nymphs developing to adults in k -th patch	0.1 (assumed)
Systemic transmission	ζ_k^L	Systemic transmission probability between infected rodents and susceptible larvae in k -th patch	$0.9 \times [0, 0.9]$ (Nonaka et al. (2010))
	ζ_k^N	Systemic transmission probability between infected rodents and susceptible nymphs in k -th patch	$0.9 \times [0, 0.9]$ (Nonaka et al. (2010))
	ζ_k^H	Systemic transmission probability between susceptible rodents and infected nymphs in k -th patch	see Section 5
Co-feeding transmission	η_k	Probability that a single larva gets infection from a single infected nymph through co-feeding transmission in k -th patch	see Section 5
Host ecology	d_k^H	Mortality rate of hosts in k -th patch	see Section 5
Host mobility	$m_{kj}(t)$	Host migration proportion from patch j to k	see Section 5

note that $\zeta_k^L m_k^L(t) \beta_k^L(t) H_k^i(t) L_k(t)$ represents the incidence term of systemic transmission route, while $\left(1 - (1 - \eta_k) N_k^i(t) / H_k(t)\right) m_k^L(t) \beta_k^L(t) H_k^s(t) L_k(t)$ and $\left(1 - (1 - \eta_k) N_k^i(t) / H_k(t)\right) (1 - \zeta_k^L) m_k^L(t) \beta_k^L(t) H_k^i(t) L_k(t)$ represent the incidence rates of co-feeding transmission routes when larvae biting susceptible and infectious hosts, respectively. To describe the co-feeding incidence through sharing a same host, feeding nymphal ticks are supposed to distribute evenly on all rodents here. Actually, the distributions of ticks on hosts may obey other complicated forms, such as Poisson distribution, which may derive other incidence terms. All parameters are positive and their descriptions are shown in Table 1. Among them, those time-dependent parameters are assumed to be continuous and $\omega = 1$ year-periodic functions.

In this model, we assume that there is no birth and death during rodents movement, and therefore, the total movement rate between immigration and emigration should satisfy

$$\sum_{k=1}^n \left(\sum_{j=1, j \neq k}^n m_{kj}(t) - \sum_{j=1, j \neq k}^n m_{jk}(t) \right) = 0.$$

Adding the equations of the host population in k -th patch, we have

$$\frac{dH_k(t)}{dt} = \sum_{j=1, j \neq k}^n m_{kj}(t)H_j(t) - \sum_{j=1, j \neq k}^n m_{jk}(t)H_k(t).$$

The host population dynamics in n -patches can be described by the following system

$$\frac{dH(t)}{dt} = M(t)H(t), \quad (2)$$

where $H(t) = (H_1(t), H_2(t), \dots, H_n(t))^T$ and the mobility matrix $M(t)$ is represented as

$$M(t) = \begin{bmatrix} -\sum_{j=1, j \neq 1}^n m_{j1}(t) & m_{12}(t) & \dots & m_{1n}(t) \\ & \ddots & \ddots & \\ m_{n1}(t) & m_{n2}(t) & \dots & -\sum_{j=1, j \neq n}^n m_{jn}(t) \end{bmatrix}.$$

We assume that the mobility matrix $M(t)$ consisting of the migration rates among various patches is irreducible. That is, the patches as vertices following the matrix $M(t)$ as arcs of a directed digraph are strongly connected under the migration of host population.

By applying Smith (1995, Remark 5.2.1), as discussed in Lou, Wu and Wu (2014), we can show that for a given nonnegative initial value for system (1), there is a unique solution which remains nonnegative for all $t \geq 0$.

Let $S_H(t) = \sum_{k=1}^n H_k(t)$ be the total density of hosts in all patches, and X be a set

$$X := \{(H_1, H_2, \dots, H_n) \in \mathbb{R}_+^n : \sum_{k=1}^n H_k > 0\}.$$

Then we get the following result:

Theorem 1 *Assume that the mobility matrix $M(t)$ is irreducible in the host migration model (2). Then model (2) has a unique positive ω -periodic solution $H^*(t) = (H_1^*(t), H_2^*(t), \dots, H_n^*(t))$ which is globally asymptotically stable to any positive solution.*

Proof Clearly, $S_H(t)$ can be determined by $\frac{dS_H(t)}{dt} = 0$, namely, $S_H(t) = S_H(0)$ which means total density of host population is a constant for all $t \geq 0$. Let $\Phi(t)$ be the fundamental solution matrix of system (2) satisfying $\frac{d\Phi(t)}{dt} = M(t)\Phi(t)$ and $\Phi(0) = I_n$ where I_n is the $n \times n$ identity matrix. Notice that $M(t)$ has nonnegative off-diagonal elements and its integral on the interval $[0, \omega]$ is irreducible. Then $\Phi(t)$ is not only $n\omega$ -periodic, but a strongly positive operator (see Smith (1995)). Then Aronsson and Kellogg (1978) implies that system (2) has a positive $n\omega$ -periodic solution $H^*(t)$ which is globally attractive for

any nonzero initial condition $H(0) \in X$. Therefore, based on the similar argument in Weng and Zhao (2011), this $n\omega$ -periodic solution is also a globally asymptotically stable ω -periodic solution satisfying $S_H^*(t) = S_H(0)$. \square

Based on this result, without loss of generality, we may assume that the rodent population density stabilizes at the periodic positive solution, $H_k^*(t)$, $k = 1, 2, \dots, n$.

Considering the population densities of nymphs $N_k(t) = N_k^s(t) + N_k^i(t)$, adult ticks $A_k(t) = A_k^s(t) + A_k^i(t)$ and rodents $H_k(t) = H_k^s(t) + H_k^i(t)$, we have the following system which is equivalent to model (1)

$$\begin{aligned}
\frac{dL_k(t)}{dt} &= \rho_k(t)A_k(t) - d_k^L(t)L_k(t) - \mu_k^L(t)L_k^2(t) - \beta_k^L(t)H_k(t)L_k(t), \\
\frac{dN_k(t)}{dt} &= m_k^L(t)\beta_k^L(t)H_k(t)L_k(t) - d_k^N(t)N_k(t) - \mu_k^N(t)N_k^2(t) - \beta_k^N(t)H_k(t)N_k(t), \\
\frac{dA_k(t)}{dt} &= m_k^N(t)\beta_k^N(t)H_k(t)N_k(t) - d_k^A(t)A_k(t) - \mu_k^A(t)A_k^2(t) - \beta_k^A(t)D_kA_k(t), \\
\frac{dN_k^i(t)}{dt} &= \zeta_k^L m_k^L(t)\beta_k^L(t)H_k^i(t)L_k(t) + \left(1 - (1 - \eta_k)^{N_k^i(t)/H_k(t)}\right) (H_k(t) - \zeta_k^L H_k^i(t)) \\
&\quad \cdot m_k^L(t)\beta_k^L(t)L_k(t) - d_k^N(t)N_k^i(t) - \mu_k^N(t)N_k(t)N_k^i(t) - \beta_k^N(t)H_k(t)N_k^i(t), \\
\frac{dH_k^i(t)}{dt} &= \zeta_k^H \beta_k^N(t)(H_k(t) - H_k^i(t))N_k^i(t) - d_k^H H_k^i(t) + \sum_{j=1, j \neq k}^n m_{kj}(t)H_j^i(t) \\
&\quad - \sum_{j=1, j \neq k}^n m_{jk}(t)H_k^i(t)
\end{aligned} \tag{3}$$

with $k = 1, 2, \dots, n$.

3 Tick population dynamics

In this section, we assume all conditions in Theorem 1 holds. Therefore, we may assume $H_k(t) = H_k^*(t)$, $k = 1, 2, \dots, n$ to study the long-term behavior of tick population dynamics. From model (3), we have a decoupled system to describe stage-structured tick population growth in k -th patch as follows:

$$\begin{aligned}
\frac{dL_k(t)}{dt} &= \rho_k(t)A_k(t) - d_k^L(t)L_k(t) - \mu_k^L(t)L_k^2(t) - \beta_k^L(t)H_k^*(t)L_k(t), \\
\frac{dN_k(t)}{dt} &= m_k^L(t)\beta_k^L(t)H_k^*(t)L_k(t) - d_k^N(t)N_k(t) - \mu_k^N(t)N_k^2(t) - \beta_k^N(t)H_k^*(t)N_k(t), \\
\frac{dA_k(t)}{dt} &= m_k^N(t)\beta_k^N(t)H_k^*(t)N_k(t) - d_k^A(t)A_k(t) - \mu_k^A(t)A_k^2(t) - \beta_k^A(t)D_kA_k(t),
\end{aligned} \tag{4}$$

for $k = 1, 2, \dots, n$.

Next, we will evaluate the net reproduction number $\mathcal{R}_T^{(k)}$ for system (4) in the k -th patch through the procedure in Wang and Zhao (2008). The linearized system of (4) in the k -th patch at the tick-free equilibrium $(0, 0, 0)$ takes the following form

$$\begin{aligned}
\frac{dL_k(t)}{dt} &= \rho_k(t)A_k(t) - (d_k^L(t) + \beta_k^L(t)H_k^*(t))L_k(t), \\
\frac{dN_k(t)}{dt} &= m_k^L(t)\beta_k^L(t)H_k^*(t)L_k(t) - (d_k^N(t) + \beta_k^N(t)H_k^*(t))N_k(t), \\
\frac{dA_k(t)}{dt} &= m_k^N(t)\beta_k^N(t)H_k^*(t)N_k(t) - (d_k^A(t) + \beta_k^A(t)D_k)A_k(t).
\end{aligned} \tag{5}$$

Obviously, system (5) is cooperative. We introduce

$$F_T^{(k)}(t) = \begin{pmatrix} 0 & 0 & \rho_k(t) \\ 0 & 0 & 0 \\ 0 & 0 & 0 \end{pmatrix},$$

and

$$V_T^{(k)}(t) = \begin{pmatrix} d_k^L(t) + \beta_k^L(t)H_k^*(t) & 0 & 0 \\ -m_k^L(t)\beta_k^L(t)H_k^*(t) & d_k^N(t) + \beta_k^N(t)H_k^*(t) & 0 \\ 0 & -m_k^N(t)\beta_k^N(t)H_k^*(t) & d_k^A(t) + \beta_k^A(t)D_k \end{pmatrix}.$$

Suppose $Y_T^{(k)}(t, s)$, $t \geq s$, is the evolution operator of the linear periodic system

$$\frac{dy}{dt} = -V_T^{(k)}(t)y.$$

That is, for each $s \in \mathbb{R}$, the evolution operator $Y_T^{(k)}(t, s)$ satisfies

$$\frac{dY_T^{(k)}(t, s)}{dt} = -V_T^{(k)}(t)Y_T^{(k)}(t, s), \quad \forall t \geq s, \quad Y_T^{(k)}(s, s) = I_3,$$

where I_3 is the 3×3 identity matrix.

Let C_ω^T be the ordered Banach space of all ω -periodic functions from \mathbb{R}^1 to \mathbb{R}^3 , equipped with the maximum norm. In the periodic patchy environment, we assume that $\phi(s) \in C_\omega^T$ represents the initial distribution of larval, nymphal and adult ticks. Then $F_T^{(k)}(s)\phi(s)$ represents the distribution of larvae produced by the adult ones who were introduced at time s in the k -th patch. Given $t \geq s$, then $Y_T^{(k)}(t, s)F_T^{(k)}(s)\phi(s)$ denotes the distribution of those ticks who were newly born into the larval tick compartment at time s and remain alive as larval, nymphal or adult ticks at time t in the k -th patch. It follows that

$$\psi(t) := \int_{-\infty}^t Y_T^{(k)}(t, s)F_T^{(k)}(s)\phi(s)ds = \int_0^\infty Y_T^{(k)}(t, t-a)F_T^{(k)}(t-a)\phi(t-a)da$$

represents the distribution of accumulative new larval, nymphal and adult ticks at time t produced by all those larval, nymphal and adult ticks $\phi(s)$ introduced at previous time to t in the k -th patch. Then, we can define a linear operator $L_T^{(k)} : C_\omega^T \rightarrow C_\omega^T$ by

$$(L_T^{(k)}\phi)(t) = \int_0^\infty Y_T^{(k)}(t, t-a)F_T^{(k)}(t-a)\phi(t-a)da, \quad \forall t \in \mathbb{R}, \quad \phi \in C_\omega^T.$$

We call $L_T^{(k)}$ the next population reproduction operator and define the net reproduction number in the k -th patch as $\mathcal{R}_T^{(k)} := \rho(L_T^{(k)})$, the spectral radius of $L_T^{(k)}$. By using theories on monotone dynamical systems (Smith 1995; Zhao 2017) and results in Wang and Zhao (2008), as discussed in Heffernan, Lou and Wu (2014) and Lou, Wu and Wu (2014), we have the following result on the tick growth in the k -th patch.

Lemma 1 *The following statements hold*

- (i) *If $\mathcal{R}_T^{(k)} \leq 1$, the tick-free equilibrium of system (4) in the k -th patch is globally asymptotically stable.*
- (ii) *If $\mathcal{R}_T^{(k)} > 1$, system (4) in the k -th patch has a unique positive ω -periodic solution $(L_k^*(t), N_k^*(t), A_k^*(t))$ which is globally asymptotically stable for every nontrivial solution.*

Without loss of generality, by relabelling each patch, we assume $\mathcal{R}_T^{(i)} \geq \mathcal{R}_T^{(j)}$ whenever $i < j$. It is natural to introduce the maximum and minimum net reproduction number for all patches:

$$\mathcal{R}_T^{max} = \max_{1 \leq k \leq n} \mathcal{R}_T^{(k)} = \mathcal{R}_T^{(1)} \quad \text{and} \quad \mathcal{R}_T^{min} = \min_{1 \leq k \leq n} \mathcal{R}_T^{(k)} = \mathcal{R}_T^{(n)}.$$

Then we have the following results.

Theorem 2 (i) *If $\mathcal{R}_T^{max} \leq 1$, the tick-free equilibrium of system (4) with n patches is globally asymptotically stable.*

- (ii) *If $\mathcal{R}_T^{min} > 1$, system (4) with n patches has a unique ω -periodic solution*

$$(L^*(t), N^*(t), A^*(t)) = (L_1^*(t), \dots, L_n^*(t), N_1^*(t), \dots, N_n^*(t), A_1^*(t), \dots, A_n^*(t)),$$

which is globally asymptotically attractive for each positive solution.

- (iii) *If $\mathcal{R}_T^{min} \leq 1 < \mathcal{R}_T^{max}$, there exists a unique K with $0 < K < n$ such that $\mathcal{R}_T^{(K)} > 1$ while $\mathcal{R}_T^{(K+1)} \leq 1$. Then system (4) with n patches satisfies*

$$\lim_{t \rightarrow \infty} (L_k(t), N_k(t), A_k(t)) = (L_k^*(t), N_k^*(t), A_k^*(t))$$

and

$$\lim_{t \rightarrow \infty} (L_p(t), N_p(t), A_p(t)) = (0, 0, 0)$$

for $1 \leq k \leq K$ and $K + 1 \leq p \leq n$.

4 The dynamics of disease spread

For a patch with the net reproduction number smaller than or equal to unity, that is $\mathcal{R}_T^{(k)} \leq 1$, there will be no ticks. For this unfavorable patch for ticks, we have $\lim_{t \rightarrow \infty} N_k^i(t) = \lim_{t \rightarrow \infty} N_k(t) = 0$ as $N_k^i(t) \leq N_k(t)$. To investigate the pathogen persistence in ticks in a habitat, we introduce another reproduction number for the pathogen. For the ease of explanation, we first investigate the scenario $\mathcal{R}_T^{min} > 1$, and then the other two cases in Theorem 2 will be discussed later. In this case, the tick population in patch k will eventually

follow the seasonal pattern $(L^*(t), N^*(t), A^*(t))$. Now consider the following asymptotic system of model (3) for infected compartments:

$$\begin{aligned} \frac{dN_k^i(t)}{dt} &= \zeta_k^L m_k^L(t) \beta_k^L(t) H_k^i(t) L_k^*(t) + \left(1 - (1 - \eta_k)^{N_k^i(t)/H_k^*(t)}\right) (H_k^*(t) - \zeta_k^L H_k^i(t)) \\ &\quad \cdot m_k^L(t) \beta_k^L(t) L_k^*(t) - d_k^N(t) N_k^i(t) - \mu_k^N(t) N_k^*(t) N_k^i(t) - \beta_k^N(t) H_k^*(t) N_k^i(t), \\ \frac{dH_k^i(t)}{dt} &= \zeta_k^H \beta_k^N(t) (H_k^*(t) - H_k^i(t)) N_k^i(t) - d_k^H H_k^i(t) + \sum_{j=1, j \neq k}^n m_{kj}(t) H_j^i(t) \\ &\quad - \sum_{j=1, j \neq k}^n m_{jk}(t) H_k^i(t), \end{aligned} \quad (6)$$

with $k = 1, 2, \dots, n$.

We will derive the basic reproduction number based on the next generation operator approach in Wang and Zhao (2008) for system (6) of periodic ordinary differential equations. Let $u(t) = (N_1^i(t), \dots, N_n^i(t), H_1^i(t), \dots, H_n^i(t))^T$ be the vector which includes all infectious variables for system (6). Linearizing system (6) at the disease-free equilibrium, we produce the following system

$$\frac{du}{dt} = (\tilde{F}(t) - \tilde{V}(t))u,$$

where

$$\tilde{F}(t) = \begin{bmatrix} \tilde{F}_{11}(t) & \tilde{F}_{12}(t) \\ \tilde{F}_{21}(t) & 0 \end{bmatrix}, \quad \tilde{V}(t) = \begin{bmatrix} \tilde{V}_{11}(t) & 0 \\ 0 & \tilde{V}_{22}(t) \end{bmatrix},$$

and

$$\begin{aligned} \tilde{F}_{11}(t) &= \begin{bmatrix} m_1^L(t) \beta_1^L(t) L_1^*(t) \ln(1 - \eta_1)^{-1} & \dots & 0 \\ & \ddots & \vdots \\ 0 & \dots & m_n^L(t) \beta_n^L(t) L_n^*(t) \ln(1 - \eta_n)^{-1} \end{bmatrix}, \\ \tilde{F}_{12}(t) &= \begin{bmatrix} \zeta_1^L m_1^L(t) \beta_1^L(t) L_1^*(t) & \dots & 0 \\ & \ddots & \vdots \\ 0 & \dots & \zeta_n^L m_n^L(t) \beta_n^L(t) L_n^*(t) \end{bmatrix}, \\ \tilde{F}_{21}(t) &= \begin{bmatrix} \zeta_1^H \beta_1^N(t) H_1^*(t) & \dots & 0 \\ & \ddots & \vdots \\ 0 & \dots & \zeta_n^H \beta_n^N(t) H_n^*(t) \end{bmatrix}, \\ \tilde{V}_{11}(t) &= \begin{bmatrix} d_1^N(t) + \mu_1^N(t) N_1^*(t) + \beta_1^N(t) H_1^*(t) & \dots & 0 \\ & \ddots & \vdots \\ 0 & \dots & d_n^N(t) + \mu_n^N(t) N_n^*(t) + \beta_n^N(t) H_n^*(t) \end{bmatrix}, \\ \tilde{V}_{22}(t) &= \begin{bmatrix} d_1^H + \sum_{j=1, j \neq 1}^n m_{j1}(t) - m_{12}(t) & \dots & -m_{1n}(t) \\ & \ddots & \vdots \\ -m_{n1}(t) & -m_{n2}(t) & \dots & d_n^H + \sum_{j=1, j \neq n}^n m_{jn}(t) \end{bmatrix}. \end{aligned}$$

Let $\tilde{Y}(t, s)$, $t \geq s$, be the evolution operator of the linear periodic system

$$\frac{dy}{dt} = -\tilde{V}(t)y.$$

For each $s \in \mathbb{R}$, the $2n \times 2n$ matrix $\tilde{Y}(t, s)$ satisfies

$$\frac{d\tilde{Y}(t, s)}{dt} = -\tilde{V}(t)Y(t, s), \quad \forall t \geq s, \quad \tilde{Y}(s, s) = I_{2n},$$

where I_{2n} is the $2n \times 2n$ identity matrix.

Let \tilde{C}_ω be the ordered Banach space of all ω -periodic functions from \mathbb{R}^1 to \mathbb{R}^{2n} equipped with the maximum norm. In the periodic patchy environment, if $\psi \in \tilde{C}_\omega$ is the initial distribution of infectious nymphs and hosts, then $\tilde{F}(s)\psi(s)$ characterizes the distribution of new infections caused by the initial infectious nymphs and hosts who were introduced at time s . Given $t \geq s$, then $\tilde{Y}(t, s)\tilde{F}(s)\psi(s)$ denotes the distribution of infectious nymphs and hosts who were newly infected at time s and remain infectious until time t . It follows that

$$\int_{-\infty}^t \tilde{Y}(t, s)\tilde{F}(s)\psi(s)ds = \int_0^\infty \tilde{Y}(t, t-a)\tilde{F}(t-a)\psi(t-a)da$$

represents the distribution of accumulative new infectious nymphs and infectious hosts at time t produced by all those infections $\psi(s)$ introduced at previous time to t . Then a linear operator $\tilde{L} : \tilde{C}_\omega \rightarrow \tilde{C}_\omega$ can be introduced as

$$(\tilde{L}\psi)(t) = \int_0^\infty Y(t, t-a)\tilde{F}(t-a)\psi(t-a)da, \quad \forall t \in \mathbb{R}, \quad \psi \in \tilde{C}_\omega.$$

Then, the basic reproduction number of the periodic system (6) is defined as

$$\mathcal{R}_0 := \rho(\tilde{L}), \quad (7)$$

the spectral radius of \tilde{L} . Based on Theorem 2.2 in Wang and Zhao (2008), the following result holds.

Lemma 2 *The zero equilibrium of system (6) is locally asymptotically stable if $\mathcal{R}_0 < 1$, and unstable if $\mathcal{R}_0 > 1$.*

Based on the observation that $N_k^i(t) \leq N_k(t)$ and $H_k^i(t) < H_k(t)$ while $\lim_{t \rightarrow \infty} [(N_k(t), H_k(t)) - (N_k^*(t), H_k^*(t))] = 0$, we have the boundedness of solutions for (6). Let

$$N^i(t) = (N_1^i(t), N_2^i(t), \dots, N_n^i(t)) \text{ and } H^i(t) = (H_1^i(t), H_2^i(t), \dots, H_n^i(t)),$$

then $u(t) = (N^i(t), H^i(t))$. System (6) takes the following form

$$\frac{du(t)}{dt} = G(t, u(t)),$$

where $G(t, u)$ is the vector field of system (6) and it is periodic in time t . In what follows, we will further show the global dynamics of system (6).

Theorem 3 *When $\mathcal{R}_T^{min} > 1$, we can use the basic reproduction number defined in (7) to characterize the global dynamics of the asymptotic system (6):*

- (i) If $\mathcal{R}_0 \leq 1$, the zero equilibrium of system (6) is globally asymptotically stable.
- (ii) If $\mathcal{R}_0 > 1$, system (6) has a unique positive ω -periodic solution $(N^{i*}(t), H^{i*}(t)) = (N_1^{i*}(t), \dots, N_n^{i*}(t), H_1^{i*}(t), \dots, H_n^{i*}(t))$, which is globally asymptotically attractive for each positive solution.

Proof For every $u \geq 0$ with $N_k^i = 0, k = 1, 2, \dots, n$, we have

$$G_k(t, u) = \zeta_k^L m_k^L(t) \beta_k^L(t) H_k^i(t) L_k^*(t) \geq 0.$$

For every $u \geq 0$ with $H_k^i = 0, k = 1, 2, \dots, n$, we have

$$G_{n+k}(t, u) = \zeta_k^H \beta_k^N(t) H_k^*(t) N_k^i(t) + \sum_{j=1, j \neq k}^n m_{kj}(t) H_j^i(t) \geq 0.$$

Let $\Gamma(t): (N^i(0), H^i(0)) \rightarrow (N^i(t), H^i(t))$ be the solution map of system (6) for $t > 0$. Then $\Gamma(\omega)$ is the Poincaré map of system (6) and $\Gamma(t)$ is monotone as the system (6) is cooperative (Smith 1995). Moreover, the irreducibility of $(\int_0^\omega M(t)dt)_{n \times n}$ implies that the semiflow of system (6) is strongly monotone.

For every $t \geq 0$ and $u \gg 0, k = 1, 2, \dots, n$, we can show that $G(t, u)$ is strictly subhomogeneous on \mathbb{R}_+^{2n} . Therefore, Theorem 3.1.2 in Zhao (2017) implies the threshold dynamics in this theorem. \square

When $\mathcal{R}_T^{min} \leq 1 < \mathcal{R}_T^{max}$, Lemma 1 implies that ticks establish in the first K patches while the remaining $n - K$ patches are unfavorable patches for ticks. In this scenario, we have an asymptotic system for the model (3)

$$\begin{aligned} \frac{dN_k^i(t)}{dt} &= \zeta_k^L m_k^L(t) \beta_k^L(t) H_k^i(t) L_k^*(t) + \left(1 - (1 - \eta_k)^{N_k^i(t)/H_k^*(t)}\right) (H_k^*(t) - \zeta_k^L H_k^i(t)) \\ &\quad \cdot m_k^L(t) \beta_k^L(t) L_k^*(t) - d_k^N(t) N_k^i(t) - \mu_k^N(t) N_k^*(t) N_k^i(t) - \beta_k^N(t) H_k^*(t) N_k^i(t), \\ \frac{dH_k^i(t)}{dt} &= \zeta_k^H \beta_k^N(t) (H_k^*(t) - H_k^i(t)) N_k^i(t) - d_k^H H_k^i(t) + \sum_{j=1, j \neq k}^n m_{kj}(t) H_j^i(t) \\ &\quad - \sum_{j=1, j \neq k}^n m_{jk}(t) H_k^i(t), \\ \frac{dH_p^i(t)}{dt} &= -d_p^H H_p^i(t) + \sum_{j=1, j \neq k}^n m_{kj}(t) H_j^i(t) - \sum_{j=1, j \neq k}^n m_{jk}(t) H_p^i(t) \end{aligned} \quad (8)$$

with $k = 1, 2, \dots, K$ and $p = K + 1, K + 2, \dots, n$. Then a similar argument as that for the system (6) can be used to define the basic reproduction number for this asymptotic system (8), denoted as $\tilde{\mathcal{R}}_0$. Furthermore, Lemma 2 and a similar result to Theorem 3 still hold.

Our next target is to characterize the global dynamics of the whole model system (3) by lifting the dynamics of the asymptotic systems with the aid of theories of internally chain transitive sets (Zhao 2017). For easy reference, we combine Lemma 1.2.1 and Theorem 1.2.1 of Zhao (2017) into the following Lemma:

Lemma 3 *Let $\mathcal{F} : \mathcal{X} \rightarrow \mathcal{X}$ be a continuous map. Then the omega limit set of any precompact positive orbit is internally chain transitive. Let \mathcal{A} be an attractor and \mathcal{C} a compact internally chain transitive set for \mathcal{F} . If $\mathcal{C} \cap W^s(\mathcal{A}) \neq \emptyset$, then $\mathcal{C} \subset \mathcal{A}$. Here, $W^s(\mathcal{A})$ is the stable set of \mathcal{A} .*

Based on this Lemma, we can establish the next result.

Theorem 4 *The following statements hold*

- (i) *If $\mathcal{R}_T^{max} \leq 1$, the zero equilibrium $(0, 0, 0, 0, 0)$ of system (3) is globally attractive.*
- (ii) *When $\mathcal{R}_T^{min} > 1$*
 - (a) *If $\mathcal{R}_0 \leq 1$, the disease-free state $(L^*(t), N^*(t), A^*(t), 0, 0)$ of system (3) is globally attractive for all nontrivial solutions.*
 - (b) *If $\mathcal{R}_0 > 1$, the unique positive ω -periodic solution $(L^*(t), N^*(t), A^*(t), N^{i*}(t), H^{i*}(t))$ of system (3) is globally attractive for each positive initial condition.*
- (iii) *When $\mathcal{R}_T^{max} > 1 \geq \mathcal{R}_T^{min}$, then*

$$\lim_{t \rightarrow \infty} (N_k(t) - N_k^*(t)) = 0 \text{ and } \lim_{t \rightarrow \infty} N_p^i(t) = \lim_{t \rightarrow \infty} N_p(t) = 0$$

for $1 \leq k \leq K$ and $K + 1 \leq p \leq n$. Furthermore, we have

- (a) *If $\tilde{\mathcal{R}}_0 \leq 1$, then $\lim_{t \rightarrow \infty} N_k^i(t) = 0$ and $\lim_{t \rightarrow \infty} H_q^i(t) = 0$ for $1 \leq k \leq K$ and $1 \leq q \leq n$;*
- (b) *If $\tilde{\mathcal{R}}_0 > 1$, then there are unique positive ω -periodic functions $N_k^{i*}(t)$ and $H_q^{i*}(t)$ such that $\lim_{t \rightarrow \infty} (N_k^i(t) - N_k^{i*}(t)) = 0$ and $\lim_{t \rightarrow \infty} (H_q^i(t) - H_q^{i*}(t)) = 0$ for $1 \leq k \leq K$ and $1 \leq q \leq n$ for all nontrivial solutions.*

Proof Let

$$P : P(L(0), N(0), A(0), N^i(0), H^i(0)) = (L(\omega), N(\omega), A(\omega), N^i(\omega), H^i(\omega))$$

be the Poincaré map of system (3). Clearly, P is compact. Let Ω be the omega limit set of $P^n(L(0), N(0), A(0), N^i(0), H^i(0))$. Then Lemma 3 implies that Ω is an internally chain transitive set for P . Next, we will prove three scenarios depending on the net reproduction number \mathcal{R}_T^{min} (or \mathcal{R}_T^{max}) and the basic reproduction number \mathcal{R}_0 .

Scenario (i): $\mathcal{R}_T^{max} \leq 1$.

From Theorem 2, tick-free equilibrium of system (4) is globally asymptotically stable. Then we have

$$\lim_{n \rightarrow \infty} P^n(L(0), N(0), A(0), N^i(0), H^i(0)) = \lim_{n \rightarrow \infty} (0, 0, 0, 0, P_5^n(H^i(0))),$$

where P_5 is the Poincaré solution map of the following system

$$\frac{dH^i(t)}{dt} = -d^H H^i(t). \quad (9)$$

That means $\Omega = \{(0, 0, 0, 0)\} \times \Omega_5$ where Ω_5 is the omega limit set of P_5 . Since 0 is globally asymptotically stable for system (9), it is easy to see that

$\Omega_5 = \{0\}$. It follows that $\Omega = \{(0, 0, 0, 0, 0)\}$. This completes the proof of the first statement (i).

Scenario (ia): $\mathcal{R}_T^{min} > 1$ and $\mathcal{R}_0 \leq 1$.

It can be seen from Theorem 2 that

$$\begin{aligned} & \lim_{n \rightarrow \infty} P^n(L(0), N(0), A(0), N^i(0), H^i(0)) \\ &= \lim_{n \rightarrow \infty} (L^*(0), N^*(0), A^*(0), \tilde{P}^n(N^i(0), H^i(0))), \end{aligned}$$

where \tilde{P} is the Poincaré solution map of system (6). It means that there exists the omega limit set $\Omega_2 \in \mathbb{R}^{2n}$ corresponding to \tilde{P} such that $\Omega = \{(L^*(0), N^*(0), A^*(0))\} \times \Omega_2$. When $\mathcal{R}_0 \leq 1$, Theorem 3 implies that for all $(L(0), N(0), A(0), N^i(0), H^i(0))$, we have

$$\lim_{n \rightarrow \infty} (\tilde{P}^n(N^i(0), H^i(0))) = (0, 0),$$

According to Lemma 3, we have $\Omega_2 = \{(0, 0)\}$. Therefore, the disease-free periodic solution $(L^*(t), N^*(t), A^*(t), 0, 0)$ of system (3) is globally attractive which completes the proof of statement (ia).

Scenario (ib): $\mathcal{R}_T^{min} > 1$ and $\mathcal{R}_0 > 1$.

In this case, the unique positive ω -periodic solution $(N^{i*}(t), H^{i*}(t))$ of system (6) is globally asymptotically stable for each positive initial condition $(N^i(0), H^i(0)) \in U(0)$ from Theorem 3. Since Ω_2 is the omega limit set of Poincaré solution map \tilde{P} , there are two possible situations

$$\Omega_2 = \{(N^{i*}(0), H^{i*}(0))\} \text{ or } \Omega_2 = \{(0, 0)\}.$$

In what follows, we will rule out the second situation $\Omega_2 = \{(0, 0)\}$.

Assume, by contradiction, that $\Omega_2 = \{(0, 0)\}$ for a positive initial condition $(N^i(0), H^i(0)) \in U(0)$. Then, $\Omega = \{(L^*(0), N^*(0), A^*(0), 0, 0)\}$ and the solution of system (3) guarantees

$$\lim_{t \rightarrow \infty} ((L(t), N(t), A(t), N^i(t), H^i(t)) - (L^*(t), N^*(t), A^*(t), 0, 0)) = 0. \quad (10)$$

Due to $\mathcal{R}_0 > 1$, there exists a small $\epsilon > 0$ such that the spectral radius of the Poincaré map associated with the following linear system

$$\begin{aligned} \frac{d\bar{N}_k^i(t)}{dt} &= [\ln(1 - \eta_k)^{-1} m_k^L(t) \beta_k^L(t) (L_k^*(t) - \epsilon) - d_k^N(t) - \mu_k^N(t) (N_k^*(t) + \epsilon) \\ &\quad - \beta_k^N(t) H_k^*(t)] \bar{N}_k^i(t) + \zeta_k^L m_k^L(t) \beta_k^L(t) (L_k^*(t) - \epsilon) \bar{H}_k^i(t), \\ \frac{d\bar{H}_k^i(t)}{dt} &= \zeta_k^H \beta_k^N(t) H_k^*(t) \bar{N}_k^i(t) - (d_k^H + \sum_{j=1, j \neq k}^n m_{jk}(t)) \bar{H}_k^i(t) \\ &\quad + \sum_{j=1, j \neq k}^n m_{kj}(t) \bar{H}_j^i(t) \end{aligned} \quad (11)$$

with $k = 1, 2, \dots, n$ is greater than one. From (10), there exists some $\tilde{t}(\epsilon) > 0$ such that $L_k(t) > L_k^*(t) - \epsilon$ and $N_k(t) < N_k^*(t) + \epsilon$ with $k = 1, 2, \dots, n$ for any $t > \tilde{t}$. For $t > \tilde{t}$, we have

$$\begin{aligned} \frac{dN_k^i(t)}{dt} &\geq \zeta_k^L m_k^L(t) \beta_k^L(t) H_k^i(t) (L_k^*(t) - \epsilon) + (1 - (1 - \eta_k)^{N_k^i(t)/H_k^*(t)}) (H_k^*(t) - \zeta_k^L H_k^i(t)) \\ &\quad \cdot m_k^L(t) \beta_k^L(t) (L_k^*(t) - \epsilon) - d_k^N(t) N_k^i(t) - \mu_k^N(t) (N_k^*(t) + \epsilon) N_k^i(t) \\ &\quad - \beta_k^N(t) H_k^*(t) N_k^i(t), \\ \frac{dH_k^i(t)}{dt} &= \zeta_k^H \beta_k^N(t) (H_k^*(t) - H_k^i(t)) N_k^i(t) - d_k^H H_k^i(t) + \sum_{j=1, j \neq k}^n m_{jk}(t) H_k^i(t) \\ &\quad + \sum_{j=1, j \neq k}^n m_{kj}(t) H_j^i(t) \end{aligned}$$

with $k = 1, 2, \dots, n$. Since system (11) is unstable, by the similar argument to Theorem 3 (ii), the following comparison system

$$\begin{aligned} \frac{d\bar{N}_k^i(t)}{dt} &= \zeta_k^L m_k^L(t) \beta_k^L(t) H_k^i(t) (L_k^*(t) - \epsilon) + (1 - (1 - \eta_k)^{N_k^i(t)/H_k^*(t)}) (H_k^*(t) - \zeta_k^L H_k^i(t)) \\ &\quad \cdot m_k^L(t) \beta_k^L(t) (L_k^*(t) - \epsilon) - d_k^N(t) N_k^i(t) - \mu_k^N(t) (N_k^*(t) + \epsilon) N_k^i(t) \\ &\quad - \beta_k^N(t) H_k^*(t) N_k^i(t), \\ \frac{d\bar{H}_k^i(t)}{dt} &= \zeta_k^H \beta_k^N(t) (H_k^*(t) - H_k^i(t)) N_k^i(t) - d_k^H H_k^i(t) + \sum_{j=1, j \neq k}^n m_{jk}(t) H_k^i(t) \\ &\quad + \sum_{j=1, j \neq k}^n m_{kj}(t) H_j^i(t) \end{aligned}$$

has a positive periodic solution

$$(\bar{N}^{i*}(t), \bar{H}^{i*}(t)) = (\bar{N}_1^{i*}(t), \dots, \bar{N}_n^{i*}(t), \bar{H}_1^{i*}(t), \dots, \bar{H}_n^{i*}(t)).$$

The comparison principle implies that

$$\liminf_{t \rightarrow \infty} ((N^i(t), H^i(t)) - (\bar{N}^{i*}(t), \bar{H}^{i*}(t))) \geq 0,$$

which contradicts to (10). Then we must have $\Omega_2 = \{(N^{i*}(0), H^{i*}(0))\}$, namely, $\Omega = \{(L^*(0), N^*(0), A^*(0), N^{i*}(0), H^{i*}(0))\}$. Therefore, statement (iib) is valid.

The statements for the remaining scenarios (iiia) and (iiib) can be shown by using similar approaches to (iia) and (iib). \square

5 Numerical illustrations

In this section, we first perform simulations on model (1) with two patches to verify theoretical results and explore the effects of migration on population dynamics.

Some baseline parameter values are taken from existing literatures studying the tick population growth and tick-borne pathogen transmission (Dunn et al.

Table 2: Different parameter values of model (1) with 2 patches. Please note that parameter values of $\rho_k(t)$ and $d_k^N(t)$ in k -th patch ($k = 1, 2$) are set to be out of phase, which implies mortality rate of nymphs is high only sometimes after the recruitment rate of larvae is high.

Parameter	Patch 1 ($k = 1$)	Patch 2 ($k = 2$)
$\rho_k(t)^{\star}$	$0.45 - 0.1 \cos(\frac{2\pi t}{365})(\text{day}^{-1})$	$0.41 - 0.1 \cos(\frac{2\pi t}{365})(\text{day}^{-1})$
$d_k^N(t)^{\star}$	$0.035 - 0.02 \sin(\frac{2\pi t}{365})(\text{day}^{-1})$	$0.03 - 0.01 \sin(\frac{2\pi t}{365})(\text{day}^{-1})$
d_k^H	$0.01(\text{day}^{-1})$	$0.03(\text{day}^{-1})$
D_k	15	20
ζ_k^L	0.5	0.25
ζ_k^I	0.5	0.25
ζ_k^H	0.5	0.3
$H_k(0)$	250	180

2013; Nonaka et al. 2010; Rosà et al. 2003; Rosà and Pugliese 2007), which are summarized in Table 1. To distinguish two patches, different parameter values are set to reflect the spatial and temporal heterogeneity in Table 2.

In Sections 3 and 4, the net reproduction number and basic reproduction number for periodic ordinary differential systems are defined as the spectral radius of operators on functional spaces. Theoretically, it is hard to derive the analytic expressions for two reproduction numbers. In this section, numerical algorithms based on Theorem 2.1 in Wang and Zhao (2008) are used to compute the reproduction numbers.

Under this scenario, the net reproduction number of tick population $\mathcal{R}_T^{min} = 1.27$ ($R_T^{(1)} = 1.56$ and $R_T^{(2)} = 1.27$) which guarantees tick population will be persistent in both patches. Moreover, we can calculate the basic reproduction number of tick-borne diseases for each patch without host migration. Fix the probability of co-feeding transmission $\eta_k = 0.04$. For the first patch, the basic reproduction number is $\mathcal{R}_0^1 = 1.88$ which is greater than 1 and then the disease will remain persistent. For the second patch, the basic reproduction number is $\mathcal{R}_0^2 = 0.61$ and the disease will die out without migration. The corresponding numerical solutions are depicted in Fig. 2(a). However, when the hosts are freely move between two patches with migration proportions $m_{12}(t) = 0.5$ and $m_{21}(t) = 0.2$, the basic reproduction number of tick-borne pathogen becomes to be greater than one, i.e., $\mathcal{R}_0 = 1.43$, indicating theoretically that the tick-borne pathogen persists in both patches, which is confirmed by the Fig. 2(b). Therefore, in this scenario, host migration promotes persistence of the pathogen transmission in a wider range. Furthermore, it is interesting to see that the amplitudes of seasonal variations of infectious hosts become larger in the first patch.

In order to explore the effects of host migrations, the relationship between the basic reproduction number and host migration proportions (m_{12} or m_{21}) is investigated in Fig. 3(a). Fixing $m_{21} = 0.2$, we can see from the blue curve that the basic reproduction number \mathcal{R}_0 is increasing with respect to m_{12} , which indicates that tick-borne pathogen will appear to be endemic in both patches

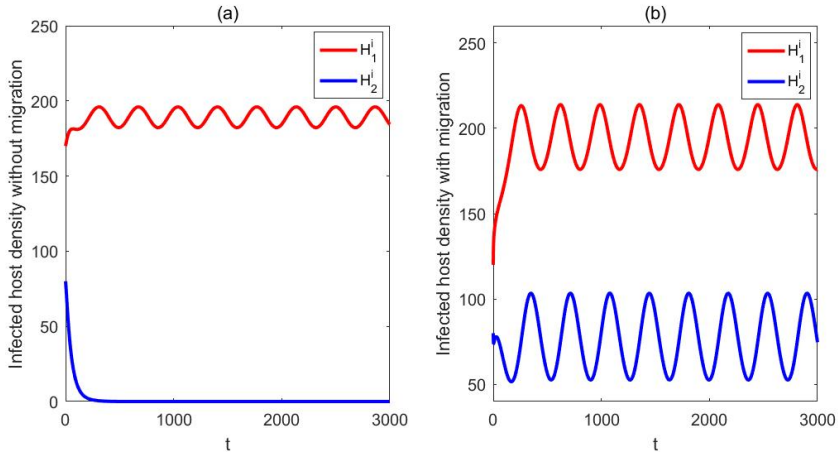


Fig. 2: Solutions of infected host population in each patch. (a) Without host migration, $H_1^i(t)$ (red dashed line) approaches to a periodic solution and $H_2^i(t)$ (blue solid line) tends to zero in the left panel. (b) When hosts are allowed to move between patches, infected host populations persist in both patches and approach to periodic solutions.

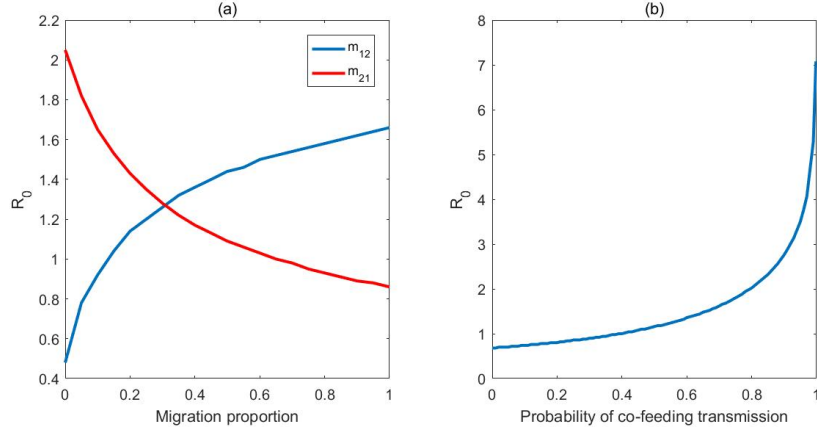


Fig. 3: The basic reproduction numbers \mathcal{R}_0 vary with the host migration proportions and probability of co-feeding transmission. (a) The blue (red) curve shows the basic reproduction number is increasing (decreasing) with respect to $m_{12} \in [0, 1]$ ($m_{21} \in [0, 1]$) when $m_{21} = 0.2$ ($m_{12} = 0.5$), $\eta_k = 0.04$ and others parameters are fixed in Table 1 and Table 2. (b) The basic reproduction number is increasing with respect to $\eta_k \in [0, 1]$ when $m_{12} = 0.15$, $m_{21} = 0.6$ and others parameters are fixed in Table 1 and Table 2.

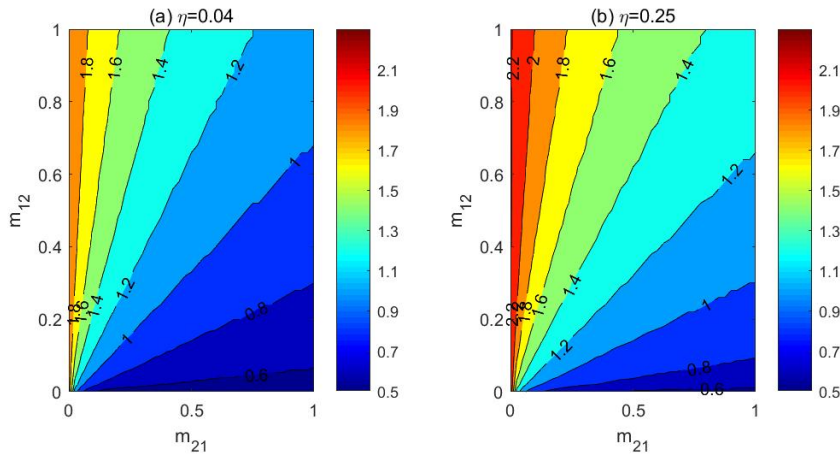


Fig. 4: The contour plots of \mathcal{R}_0 depending on the host migration proportions m_{12} , m_{21} with different co-feeding transmission probability (a) $\eta_k = 0.04$ and (b) $\eta_k = 0.25$ when the other parameters are fixed in Table 1 and Table 2.

once the host migration proportion from patch 2 to 1 is greater than 0.12. Then we set $m_{12} = 0.5$ and investigate the effect of host migration proportion m_{21} on the basic reproduction number. The red curve shows that basic reproduction number \mathcal{R}_0 is decreasing with the increasing of host migration proportion m_{21} . Furthermore, the influence of co-feeding transmission on the basic reproduction number is illustrated in Fig. 3(b) when $m_{12} = 0.15$ and $m_{21} = 0.6$ are fixed. From Fig. 3(b), the increasing of co-feeding transmission makes a greater contribution to the spread of tick-borne diseases.

Fig. 4 presents contour plots for the basic reproduction number versus the migration proportions $m_{12}, m_{21} \in [0, 1]$ when the co-feeding transmission probabilities are $\eta_k = 0.04$ and $\eta_k = 0.25$ respectively. It is easy to observe that the isolines move towards bottom right corner and dark red color area appears in the upper left corner while the probability of co-feeding transmission η_k increases from 0.04 to 0.25. From Fig. 4, we can see the parameter region satisfying $\mathcal{R}_0 > 1$ becomes larger when co-feeding transmission probability increases.

To better understand the effect of host migration on population persistence and disease spreading, simulations for 9 patches, P_1, P_2, \dots, P_9 , are performed. The movement rates are used to reflect the distributions of patches and the relative distances among them. In this case, all movement rates are set to be periodic. To reflect the variety of patches and generality of theoretical frameworks in this study, 9 patches are categorized into three classes: 5 patches (P_1, P_2, \dots, P_5) with net reproduction number and basic reproduction number both greater than one, two patches (P_6 and P_7) with net reproduction number more than one and basic reproduction number less than one, and two patches (P_8 and P_9) with net reproduction number less than

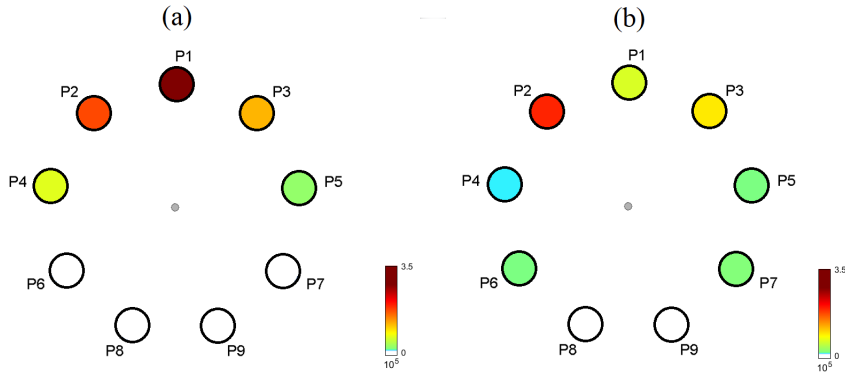


Fig. 5: The comparison of accumulated infected nymph density for model (3) in a year: (a) 9 patches are isolated from each other; (b) host population can move freely among 9 patches.

one. Then there is no disease risk in patches $P_6 - P_9$ (see Fig. 5(a) for the accumulated yearly amounts of infected nymphal ticks). When host species are freely moving among 9 patches with parameters listed in the Appendix Section, then accumulated yearly amounts of infected nymphal ticks for each patch P_i , $i = 1, 2, \dots, 9$ can be simulated as Fig. 5(b) (also presented in the Appendix Section). In this case, the basic reproduction number for the whole 9 patches is $\mathcal{R}_0 = 2.05$ which illustrates that tick-borne pathogen can spread. However for the patches with net reproduction numbers smaller than one (P_8 and P_9), the pathogen transmission cycle is not established and there is no disease risk. This confirms the results in Theorem 4. Migration can reduce the severity of tick-borne diseases dramatically for some patches, such as the first patch P_1 where the accumulated infected nymph number decreases from 3.5098×10^5 to 5.694×10^4 . At the same time, migration may facilitate the establishment of pathogen spreading in those patches with the patch basic reproduction number smaller than one, such as P_6 and P_7 . However, since the net reproduction numbers for P_8 and P_9 are both less than one, the pathogen fails to persist even with the help of infected host species migration. The last column of Table 6 in the Appendix Section lists the comparison of accumulated yearly nymphal ticks and infected nymphal ticks across 9 patches for Fig. 5(a) and (b), each corresponding to with and without host migration.

6 Discussions

Habitat fragmentation, a process of slowly altering the layout of the physical environment, may cause serious consequences on population dynamics. The current study evaluates the effect of spatial heterogeneity and host spatial movement on tick-borne pathogen transmission. In addition to that, seasonal factors on tick growth and co-feeding transmission factor are incorporated.

Since the range tick population moves by itself is limited, the model is to uncover the relationship between rodent population dispersal and the spread of tick-borne diseases.

Unlike existing models involving many variables, this paper proposes a periodic tick-borne disease model with less variables in the consideration of patchy environment and co-feeding transmissions. Based on feeding behaviour of tick population, ticks are stratified into three stages: larvae, nymphs and adults. In modeling the co-feeding transmission, nymphs are assumed to obey uniform distribution on rodent population at time t . The global dynamics of tick population in each patch can be characterized by the net reproduction numbers \mathcal{R}_T^{max} and \mathcal{R}_T^{min} which can guarantee that tick-free equilibrium and the unique ω -periodic solution with n patches are globally asymptotically stable, respectively. Furthermore, the basic reproduction number of tick-borne disease \mathcal{R}_0 is derived and the tick-borne disease transmission pattern is investigated through the theory of monotone dynamics systems. Further numerical simulations are performed to show that rodent migration can promote the disease spreading among all patches. This interesting result inspires us that migration restriction of host population among multiple patches can be used to control the breakout and spread of tick-borne disease.

Co-feeding transmission is another key factor which may make a significant contribution to the pathogen spread. The co-feeding transmission incidence term is formulated in the current model (1) by a uniform distribution assumption, that is, feeding nymphal ticks are supposed to distribute evenly on all rodents. The term of the probability of co-feeding transmission in tick-borne disease model (1) should be reformulated with other distribution assumptions, which will be our future work.

Another interesting aspect worthy to be investigated is the host immune response in the tick-borne disease transmission cycle. First, the host immune response to tick infestation may regulate the tick population dynamics. Many interesting models have been formulated to include the effect of this density-dependent aspect, for example, the models in Fan, Thieme and Zhu (2015) and Rosà et al. (2003). This would be especially important to evaluate the effect of co-feeding since when many ticks are biting a single host, the density-dependent death of ticks due to host grooming should be counted. The current paper incorporates the host immunity to tick biting by density-dependent death rates of ticks. However, other types of self-regulations due to host immunity may be possible. Moreover, existing studies show that various types of host immune effector mechanisms could be induced by tick-borne pathogen (Torina et al. 2020). It would be interesting to include the effect of host immune response to infection with tick-transmitted pathogen in model formulation. However the modeling process involves careful biological justifications, and possible immunological- and epidemiological- modeling frameworks can be used.

Table 3: Different parameter values of model (1) with 9 patches.

Patch	ρ_k	η_k^L	β_k^L	β_k^N	$H_k(0)$
P_1	$0.6 - 0.04 \cos(2\pi t/365)$	0.45	0.0015	0.0015	230
P_2	$0.51 - 0.06 \cos(2\pi t/365)$	0.35	0.0012	0.0012	250
P_3	$0.46 - 0.1 \cos(2\pi t/365)$	0.4	0.0009	0.0009	220
P_4	$0.43 - 0.1 \cos(2\pi t/365)$	0.28	0.00087	0.00087	250
P_5	$0.45 - 0.1 \cos(2\pi t/365)$	0.3	0.0012	0.0012	230
P_6	$0.38 - 0.1 \cos(2\pi t/365)$	0.32	0.00039	0.00039	230
P_7	$0.42 - 0.05 \cos(2\pi t/365)$	0.2	0.0006	0.0006	200
P_8	$0.21 - 0.05 \cos(2\pi t/365)$	0.1	0.0009	0.0009	180
P_9	$0.25 - 0.05 \cos(2\pi t/365)$	0.05	0.00045	0.00045	200

Acknowledgements This work was supported by the Natural Science Foundation of China (No. 11701072). We are very grateful to the anonymous referees for careful reading and valuable comments that significantly improve our manuscript.

Appendix

We show parameter values used in Fig.5, including recruitment rates of larval ticks ρ_k , probability of co-feeding transmission η_k , systemic transmission probability between infected rodents and susceptible larvae ζ_k^L and between susceptible rodents and infected nymphs ζ_k^H , and initial rodent densities $H_k(0)$ in Table 3. Host migration proportions from patch j to patch k take the form $m_{kj}(t) = (m_{kj}^{(1)} m_{kj}^{(2)})(1 - \cos(2\pi t/365))^T$, $j, k = 1, 2, \dots, 9$. Table 4 lists all the components $m_{kj}^{(1)}$ and $m_{kj}^{(2)}$ of host migration proportions. Other parameters among the 9 patches are fixed at the same values as follows:

$$\begin{aligned}
 d_k^L = 0.01, \quad d_k^N &= \begin{cases} 0.03 - 0.01 \sin(2\pi t/365), & k = 1, 2, 3, 4, \\ 0.02 - 0.01 \sin(2\pi t/365), & k = 5, 6, 7, 8, 9, \end{cases} \\
 d_k^A = 0.00625, \quad d_k^H = 0.01, \quad \mu_k^L = \mu_k^N = \mu_k^A &= 0.00001, \\
 \zeta_k^L = 0.5, \quad \zeta_k^N = 0.5, \quad \zeta_k^H = 0.57, \\
 m_k^L = 0.35, \quad m_k^N = 0.1, \quad D_k = 20.
 \end{aligned}$$

Without migration, we calculate the net reproduction numbers, the basic reproduction numbers and accumulated infected nymphal densities in one year for each patch k , $k = 1, 2, \dots, 9$ and list them in Table 5. When host migration is considered, the added numbers of accumulated yearly nymphal ticks and infected nymphal ticks across 9 patches are summarized in Table 6.

References

- Allen LJS, Bolker BM, Lou Y, Neve AL (2007) Asymptotic profiles of the steady states for an SIS epidemic patch model. *SIAM J App Math* 67(5): 1283-1309
- Arino J, Davis JR, Hartley D, Jordan R, Miller JM, van den Driessche P (2005) A multi-species epidemic model with spatial dynamics. *Math Med Biol* 22(2): 129-142

Table 4: Parameter values of host migration proportion $(m_{kj}^{(1)} \ m_{kj}^{(2)})^T$.

$k \backslash j$	P_1	P_2	P_3	P_4	P_5	P_6	P_7	P_8	P_9
P_1	—	$\begin{pmatrix} 0.5 \\ -0.05 \end{pmatrix}$	$\begin{pmatrix} 0.7 \\ -0.06 \end{pmatrix}$	$\begin{pmatrix} 0.65 \\ -0.05 \end{pmatrix}$	$\begin{pmatrix} 0.75 \\ -0.04 \end{pmatrix}$	$\begin{pmatrix} 0.62 \\ -0.08 \end{pmatrix}$	$\begin{pmatrix} 0.5 \\ -0.03 \end{pmatrix}$	$\begin{pmatrix} 0.38 \\ -0.05 \end{pmatrix}$	$\begin{pmatrix} 0.59 \\ -0.05 \end{pmatrix}$
P_2	$\begin{pmatrix} 0.45 \\ -0.07 \end{pmatrix}$	—	$\begin{pmatrix} 0.39 \\ -0.1 \end{pmatrix}$	$\begin{pmatrix} 0.29 \\ -0.05 \end{pmatrix}$	$\begin{pmatrix} 0.15 \\ -0.02 \end{pmatrix}$	$\begin{pmatrix} 0.58 \\ -0.09 \end{pmatrix}$	$\begin{pmatrix} 0.75 \\ -0.07 \end{pmatrix}$	$\begin{pmatrix} 0.21 \\ -0.05 \end{pmatrix}$	$\begin{pmatrix} 0.18 \\ -0.05 \end{pmatrix}$
P_3	$\begin{pmatrix} 0.26 \\ -0.03 \end{pmatrix}$	$\begin{pmatrix} 0.25 \\ -0.04 \end{pmatrix}$	—	$\begin{pmatrix} 0.32 \\ -0.05 \end{pmatrix}$	$\begin{pmatrix} 0.47 \\ 0.05 \end{pmatrix}$	$\begin{pmatrix} 0.18 \\ -0.08 \end{pmatrix}$	$\begin{pmatrix} 0.44 \\ -0.07 \end{pmatrix}$	$\begin{pmatrix} 0.5 \\ -0.06 \end{pmatrix}$	$\begin{pmatrix} 0.47 \\ -0.05 \end{pmatrix}$
P_4	$\begin{pmatrix} 0.87 \\ 0.03 \end{pmatrix}$	$\begin{pmatrix} 0.61 \\ 0.06 \end{pmatrix}$	$\begin{pmatrix} 0.24 \\ 0.08 \end{pmatrix}$	—	$\begin{pmatrix} 0.5 \\ -0.05 \end{pmatrix}$	$\begin{pmatrix} 0.31 \\ 0.08 \end{pmatrix}$	$\begin{pmatrix} 0.4 \\ -0.1 \end{pmatrix}$	$\begin{pmatrix} 0.3 \\ -0.03 \end{pmatrix}$	$\begin{pmatrix} 0.14 \\ -0.03 \end{pmatrix}$
P_5	$\begin{pmatrix} 0.33 \\ -0.07 \end{pmatrix}$	$\begin{pmatrix} 0.37 \\ -0.05 \end{pmatrix}$	$\begin{pmatrix} 0.13 \\ -0.03 \end{pmatrix}$	$\begin{pmatrix} 0.2 \\ 0.05 \end{pmatrix}$	—	$\begin{pmatrix} 0.34 \\ 0.1 \end{pmatrix}$	$\begin{pmatrix} 0.25 \\ -0.06 \end{pmatrix}$	$\begin{pmatrix} 0.12 \\ 0.04 \end{pmatrix}$	$\begin{pmatrix} 0.36 \\ -0.05 \end{pmatrix}$
P_6	$\begin{pmatrix} 0.21 \\ -0.13 \end{pmatrix}$	$\begin{pmatrix} 0.6 \\ 0.05 \end{pmatrix}$	$\begin{pmatrix} 0.49 \\ 0.21 \end{pmatrix}$	$\begin{pmatrix} 0.52 \\ 0.17 \end{pmatrix}$	$\begin{pmatrix} 0.25 \\ 0.11 \end{pmatrix}$	—	$\begin{pmatrix} 0.33 \\ 0.11 \end{pmatrix}$	$\begin{pmatrix} 0.09 \\ 0.02 \end{pmatrix}$	$\begin{pmatrix} 0.27 \\ -0.05 \end{pmatrix}$
P_7	$\begin{pmatrix} 0.32 \\ -0.12 \end{pmatrix}$	$\begin{pmatrix} 0.65 \\ -0.03 \end{pmatrix}$	$\begin{pmatrix} 0.15 \\ -0.05 \end{pmatrix}$	$\begin{pmatrix} 0.26 \\ -0.06 \end{pmatrix}$	$\begin{pmatrix} 0.3 \\ 0.02 \end{pmatrix}$	$\begin{pmatrix} 0.24 \\ 0.12 \end{pmatrix}$	—	$\begin{pmatrix} 0.2 \\ -0.07 \end{pmatrix}$	$\begin{pmatrix} 0.16 \\ -0.03 \end{pmatrix}$
P_8	$\begin{pmatrix} 0.12 \\ -0.05 \end{pmatrix}$	$\begin{pmatrix} 0.2 \\ -0.1 \end{pmatrix}$	$\begin{pmatrix} 0.1 \\ -0.05 \end{pmatrix}$	$\begin{pmatrix} 0.07 \\ 0.03 \end{pmatrix}$	$\begin{pmatrix} 0.006 \\ 0.004 \end{pmatrix}$	$\begin{pmatrix} 0.44 \\ 0.18 \end{pmatrix}$	$\begin{pmatrix} 0.1 \\ -0.02 \end{pmatrix}$	—	$\begin{pmatrix} 0.22 \\ -0.09 \end{pmatrix}$
P_9	$\begin{pmatrix} 0.35 \\ -0.05 \end{pmatrix}$	$\begin{pmatrix} 0.18 \\ -0.07 \end{pmatrix}$	$\begin{pmatrix} 0.26 \\ -0.02 \end{pmatrix}$	$\begin{pmatrix} 0.44 \\ -0.02 \end{pmatrix}$	$\begin{pmatrix} 0.35 \\ -0.05 \end{pmatrix}$	$\begin{pmatrix} 0.49 \\ -0.05 \end{pmatrix}$	$\begin{pmatrix} 0.13 \\ -0.05 \end{pmatrix}$	$\begin{pmatrix} 0.29 \\ -0.1 \end{pmatrix}$	—

Table 5: Net reproduction numbers and basic reproduction numbers for 9 patches.

	P_1	P_2	P_3	P_4	P_5	P_6	P_7	P_8	P_9
\mathcal{R}_T	2.12	1.83	1.61	1.44	1.48	1.34	1.34	0.65	0.86
\mathcal{R}_0	2.47	1.92	1.64	1.36	1.8	0.88	0.95	not defined	not defined

Table 6: Accumulated yearly nymphal ticks (AYNT) and accumulated yearly infected nymphal ticks (AYINT) with and without migration, and their comparisons for 9 patches ($\times 10^5$).

	Without migration		With migration		Comparisons	
	AYNT	AYINT	AYNT	AYINT	AYNT	AYINT
P_1	3.6599	3.5098	0.5973	0.5694	-3.0626	-2.9404
P_2	2.3746	1.7109	2.4389	1.8927	0.0643	0.1818
P_3	1.7637	1.1409	1.7451	0.8656	-0.0186	-0.2753
P_4	1.0794	0.2164	0.8644	0.0773	-0.2150	-0.1391
P_5	1.2771	0.6064	1.0947	0.4834	-0.1824	-0.1230
P_6	0.8382	0.0000	0.8194	0.1034	-0.0188	0.1034
P_7	0.9296	0.0000	0.8208	0.1261	-0.1088	0.1261
P_8	0.0000	0.0000	0.0000	0.0000	0.0000	0.0000
P_9	0.0000	0.0000	0.0000	0.0000	0.0000	0.0000
Total number	11.9225	7.1844	8.3806	4.1179	-3.5419	-3.0665

- Aronsson G, Kellogg RB (1978) On a differential equation arising from compartmental analysis. *Math Biosci* 38(1-2): 113-122
- Centers for Disease Control and Prevention. Recent Surveillance Data. <https://www.cdc.gov/lyme/datasurveillance/recent-surveillance-data.html>
- Dennis DT, Nekomoto TS, Victor JC, Paul WS, Piesman J (1998) Reported distribution of *Ixodes scapularis* and *Ixodes pacificus* (*Acarini: Ixodidae*) in the United States. *J Med Entomol* 35(5): 629-638
- Dunn JM, Davis S, Stacey A, Diuk-Wasser MA (2013) A simple model for the establishment of tick-borne pathogens of *Ixodes scapularis*: A global sensitivity analysis of \mathcal{R}_0 . *J Theor Biol* 335: 213-221
- Egyed L, Élő P, Sréter-Lancz Z, Széll Z, Balogh Z, Sréter T (2012) Seasonal activity and tick-borne pathogen infection rates of *Ixodes ricinus* ticks in Hungary. *Ticks Tick Borne Dis* 3(2): 90-94
- Fan G, Thieme HR and Zhu H (2015) Delay differential systems for tick population dynamics. *J Math Biol* 71(5): 1017-1048
- Gao D, Ruan S (2011) An SIS patch model with variable transmission coefficients. *Math Biosci* 232(2): 110-115
- Hancock PA, Brackley R, Palmer SCF (2011) Modelling the effect of temperature variation on the seasonal dynamics of *Ixodes ricinus* tick populations. *Int J Parasitol* 41(5): 513-522
- Heffernan JM, Lou Y, Wu J (2014) Range expansion of *Ixodes Scapularis* Tick and of *Borrelia Burgdorferi* by Migratory birds. *Discrete Contin Dyn Syst Ser. B* 19(10): 3147-3167
- Hudson PJ, Norman RA, Laurenson MK, Newborn D, Gaunt M, Jones L, Reid H, Gould D, Bowers R, Dobson A (1995) Persistence and transmission of tick-borne viruses: *Ixodes ricinus* and louping-ill virus in red grouse populations. *Parasitology* 111 Suppl(S1): 49-58
- Kurtenbach K, Hanincová K, Tsao JI, Margos G, Fish D, Nicholas H (2006) Fundamental processes in the evolutionary ecology of Lyme *borreliosis*. *Nat Rev Microbiol* 4(9): 660-669
- Liu K, Lou Y, Wu J (2017) Analysis of an age structured model for tick populations subject to seasonal effects. *J Differ Equations* 263(4): 2078-2112
- Lou Y, Wu J, Wu X (2014) Impact of biodiversity and seasonality on Lyme-pathogen transmission. *Theor Biol Med Model* 11(1): 50
- Lou Y, Wu J (2017) Modeling Lyme disease transmission. *Infect Dis Model* 2(2): 229-243
- Nah K, Magpantay FMG, Bede-Fazekas Á, Rost G, Trájer AJ, Wu X, Zhang X, Wu J (2019) Assessing systemic and non-systemic transmission risk of tick-borne encephalitis virus in Hungary. *PloS one* 14(6): e0217206
- Nonaka E, Ebel GD, Wearing HJ (2010) Persistence of pathogens with short infectious periods in seasonal tick populations: the relative importance of three transmission routes. *PLoS one* 5(7): e11745
- O'Connell S (2010) Lyme *borreliosis*: current issues in diagnosis and management. *Curr Opin Infect Dis* 23(3): 231-235
- Ogden NH, Lindsay LR, Morshed M, Sockett PN, Artsob H (2009) The emergence of Lyme disease in Canada. *Can Med Assoc J* 180(12): 1221-1224
- Ogden NH, Koffi JK, Lindsay LR, Fleming S, Mombourquett DC, Sanford C, Badcock J, Gad RR, Jain-Sheehan N, Moore S, Russell C, Hobbs L, Baydack R, Graham-Derham S, Lachance L, Simmonds K, Scott AN (2015) Surveillance for Lyme disease in Canada, 2009 to 2012. *Can Commun Dis Rep* 41(6): 132-145
- Ostfeld R (2010) *Lyme Disease: The Ecology of A Complex System*. Oxford University Press, New York
- Pettersson JH, Golovljova I, Vene S, Jaenson TG (2014) Prevalence of tick-borne encephalitis virus in *Ixodes ricinus* ticks in northern Europe with particular reference to Southern Sweden. *Parasite Vector* 7(1): 102
- Randolph SE, Rogers DJ (1997) A generic population model for the African tick *Rhipicephalus appendiculatus*. *Parasitology* 115: 265-279
- Rosà R, Pugliese A, Norman R, Hudson PJ (2003) Thresholds for disease persistence in models for tick-borne infections including non-viraemic transmission, extended feeding

- and tick aggregation. *J Theor Biol* 224(3): 359-376
- Rosà R, Pugliese A (2007) Effects of tick population dynamics and host densities on the persistence of tick-borne infections. *Math Biosci* 208(1): 216-240
- Smith HL (1995) Monotone dynamical systems: an introduction to the theory of competitive and cooperative systems. *ams ebooks program* 41(5):174
- Torina A, Villari S, Blanda V, et al. (2020) Innate immune response to tick-borne pathogens: Cellular and molecular mechanisms induced in the hosts. *Int J Mol Sci* 21(15): 5437
- Voordouw MJ (2015) Co-feeding transmission in Lyme disease pathogens. *Parasitology* 142(2): 290-302
- Wang W, Mulone G (2003) Threshold of disease transmission in a patch environment. *J Math Anal Appl* 285(1): 321-335
- Wang W, Zhao X-Q (2008) Threshold dynamics for compartmental epidemic models in periodic environments. *J Dyn Differ Equ* 20(3): 699-717
- Weng P, Zhao X-Q (2011) Spatial dynamics of a nonlocal and delayed population model in a periodic habitat. *Discrete Contin Dyn Syst Ser A* 29(1): 343-366
- Wu X, Magpantay FMG, Wu J, Zou X (2015) Stage-structured population systems with temporally periodic delay. *Math Methods Appl Sci* 38(16): 3464-3481
- Zhao X-Q (2012) Global dynamics of a reaction and diffusion model for Lyme disease. *J Math Biol* 65(4): 787-808
- Zhao X-Q (2017) *Dynamical systems in population biology*. Springer-Verlag, New York